COLD SPRING HARBOR
Molecular Case Studies

RESEARCH REPORT

A de novo start-loss in *EFTUD2* associated with mandibulofacial dysostosis with microcephaly: case report

Muhammad Kohailan,[1] Omayma Al-Saei,[2] Sujitha Padmajeya,[2] Waleed Aamer,[2] Najwa Elbashir,[2] Ammira Al-Shabeeb Akil,[2] Abdul-Rauf Kamboh,[3] and Khalid Fakhro[1,2,4]

[1]College of Health and Life Sciences, Hamad Bin Khalifa University, Doha 34110, Qatar; [2]Department of Human Genetics, [3]Department of Pediatric Ophthalmology, Sidra Medicine, Doha 26999, Qatar; [4]Department of Genetic Medicine, Weill-Cornell Medical College, Doha 24144, Qatar

Abstract Mandibulofacial dysostosis with microcephaly (MFDM) is a rare genetic disorder inherited in an autosomal dominant pattern. Major characteristics include developmental delay, craniofacial malformations such as malar and mandibular hypoplasia, and ear anomalies. Here, we report a 4.5-yr-old female patient with symptoms fitting MFDM. Using whole-genome sequencing, we identified a de novo start-codon loss (c.3G > T) in the *EFTUD2*. We examined *EFTUD2* expression in the patient by RNA sequencing and observed a notable functional consequence of the variant on gene expression in the patient. We identified a novel variant for the development of MFDM in humans. To the best of our knowledge, this is the first report of a start-codon loss in *EFTUD2* associated with MFDM.

Corresponding author:
kfakhro@sidra.org

Ontology terms:
mandibulofacial dysostosis; microcephaly

Published by Cold Spring Harbor Laboratory Press

doi:10.1101/mcs.a006206

INTRODUCTION

Mandibulofacial dysostosis with microcephaly (MFDM; also known as Guion-Almeida type; MIM #610536) is a rare autosomal dominant disorder characterized by developmental delay and several craniofacial malformations, including micrognathia, malar hypoplasia, ear anomalies, microcephaly, cleft palate, and facial asymmetry. In some cases, involvement of other organs have been reported, such as thumb anomalies, heart defects, esophageal atresia, and renal malformations (Guion-Almeida et al. 2006; Wieczorek et al. 2007; Guion-Almeida et al. 2009; Wieczorek et al. 2009). Patients may also present with eye abnormalities, including microphthalmia, microcornea, coloboma, and myopia (Deml et al. 2015).

From a total of 119 previously reported MFDM patients in the literature (Huang et al. 2016; Matsuo et al. 2017; Rengasamy Venugopalan et al. 2017; Yu et al. 2018; Lacour et al. 2019; Silva et al. 2019; Jacob et al. 2020; Kim et al. 2020; Narumi-Kishimoto et al. 2020; Xu et al. 2021a; Li et al. 2022), 95 cases (80%) were found to harbor deleterious variants in *Elongation Factor Tu GTP Binding Domain Containing 2* gene (*EFTUD2*; MIM #603892). In 76 cases both parents were also genotyped, and 60 (79%) were found to have de novo variants. The remaining were either germline mosaic or inherited in an autosomal dominant manner (Huang et al. 2016). The human *EFTUD2* encodes the U5-116kD nuclear protein, which plays a critical role in the pre-mRNA splicing process (Fabrizio et al. 1997). Recent

in vivo experiments performed on mutant mice showed the effect of *eftud2* knockdown on the differential splicing of Mdm2 and activation of P53 in neural crest cells, which in turn led to craniofacial defects (Beauchamp et al. 2021).

More than 90 pathogenic variants in *EFTUD2* have been reported to date. These vary in impact on the 29-exon gene, perturbing gene function by affecting protein interaction, stability, conformation, localization, and/or post-translational modifications (Huang et al. 2016; Matsuo et al. 2017; Rengasamy Venugopalan et al. 2017; Yu et al. 2018; Lacour et al. 2019; Silva et al. 2019; Jacob et al. 2020; Kim et al. 2020; Narumi-Kishimoto et al. 2020; Xu et al. 2021a; Li et al. 2022). The types of variants reported include deletions, duplications, missense, splice site, and stop-gain mutations. However, no start-loss variants have been previously reported in human MFDM patients.

Here, we report the first case of a start-loss in *EFTUD2* causing disease. We discovered this by whole-genome sequencing (WGS), confirmed segregation in the family by Sanger sequencing, and followed up with assessing gene expression levels to confirm functional effect.

RESULTS

Clinical Presentation and Family History

Here, we report a 4.5-yr-old female patient of South Asian ancestry, enrolled as part of the Qatar Mendelian Disease Program (Fakhro et al. 2019), who presented mainly with craniofacial features including micrognathia, malar hypoplasia, right microtia, right hemifacial microsomia, cleft palate, and a limitation in mouth opening (jaw opens to the rightward). The patient was initially diagnosed also with microphthalmia, but upon reexamination, it turns out to be mild ptosis. Eye testing also revealed right intermittent exotropia, normal stereo test, and right amblyopia (logmar: right = 0.3, left = 0.1) that was treated later with occlusion therapy. Other developmental features included conductive hearing loss, auditory atresia, congenital microcephaly with normal magnetic resonance imaging (MRI) brain, poor weight gain, and speech delay that was being treated by speech therapy (Table 1).

The patient was first referred to the ophthalmology clinic for eye consultation, which includes the examination of the anterior segment, pupil, dilation and refraction, and optic nerve and fundus. The genetic testing was requested upon the initial diagnosis with microphthalmia. She was then referred to the pediatrician to screen for allergies and to the ear, nose, and throat (ENT) clinic for physical tests. Audiology evaluation by otoscopy and tympanometry was also performed. The patient was then referred to a speech therapist for oral motor assessment. Upon these multiclinic assessments, the patient and her family (parents and unaffected sister) were enrolled for WGS to identify the genetic etiology underlying her syndromic presentation. The absence of family history of disease and the lack of parental consanguinity suggested that a de novo variant caused this condition.

Genomic Analyses

We first applied our optimized laboratory processing pipelines that look for recessive mutations (Al-Kurbi et al. 2022) and structural variants (E Aliyev, A Visconti, N Syed, et al., unpubl.), but we did not find any candidate variants that could be linked to the presented disease phenotype. We then used a combinatorial approach for de novo mutation calling that leverages three separate underlying approaches to identify 92 high genotype quality de novo variants. Focusing on protein-altering variants that were predicted damaging, we discovered one variant of particular interest in the *EFTUD2* (ClinVar accession number

Table 1. Clinical features of the patient in our study, compared to the spectrum of findings in all reported cases of MFDM

Features	This study	All reported cases[a]	Estimated prevalence (%)
Craniofacial			
Micrognathia	Yes	93/95	98
Small or dysplastic pinna(e)	Yes	90/93	97
Malar hypoplasia	Yes	84/90	93
Hearing loss	Yes	75/89	84
Conductive	Yes	33/55	60
Mixed	No	15/55	27
Sensorineural	No	7/55	13
Auditory atresia/stenosis	Yes	50/78	64
Vestibular system abnormalities[b]	NR	16/28	57
Ossicular abnormalities[b]	NR	11/19	58
Microphthalmia[b]	No	10/32	31
Facial asymmetry	Yes	29/52	56
Preauricular tag(s)	No	46/91	51
Cleft palate	Yes	45/94	48
Choanal atresia	No	27/89	30
Neonatal resuscitation	No	14/48	29
Tracheostomy	No	11/54	20
Limitation of mouth opening	Yes	9/86	10
Extracranial			
Thumb anomalies	No	25/83	30
Heart defects	No	29/95	31
Esophageal atresia	No	24/91	26
Renal malformation	No	9/87	10
Development			
Developmental delay	Yes	89/89	100
Microcephaly	Yes	84/95	88
Congenital	Yes	36/57	63
Postnatal	No	21/57	37
Epileptic seizures	No	23/83	28

[a]Obtained from Deml et al. (2015; PMID: 26118977), Huang et al. (2016; PMID: 26507355), Yu et al. (2018; PMID: 29381487), Narumi-Kishimoto et al. (2020; PMID: 32541334), Jacob et al. (2020; PMID: 32943010), and this study.
[b]These features were not reported in several studies, and thus the prevalence estimates are not accurate.

Table 2. The identified de novo variant in the patient

Gene	Chromosome (hg19)	HGVS DNA reference	HGVS protein reference	Variant type	Predicted effect	Zygosity
EFTUD2	17:42971887	c.3G > T	p.(Met1?)	Substitution	Start loss	Heterozygous

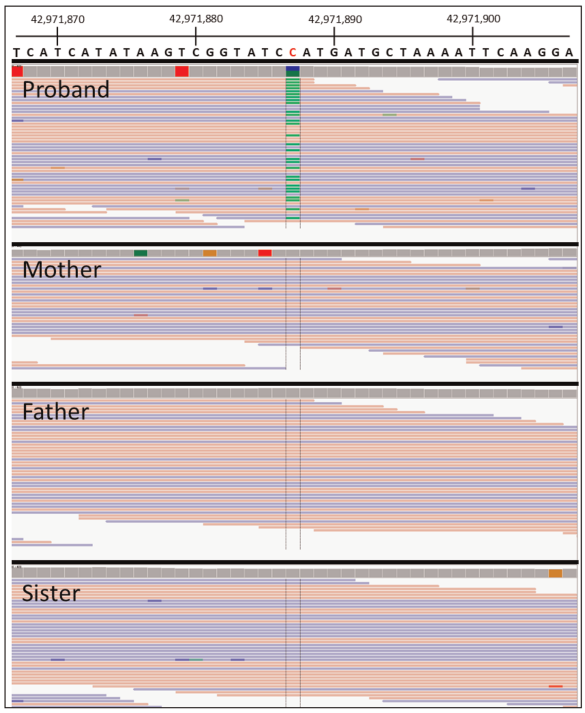

Figure 1. Integrative Genomics Viewer (IGV) visualization of the *EFTUD2* variant. The variant allele (A; light green bands) occurs in a heterozygous state and replaces the wild-type C nucleotide.

SCV002499764), previously implicated in MFDM clinical phenotypes (Table 2). This patient's variant was predicted to cause a loss of function because of removal of the start codon of *EFTUD2* (c.3G > T, p.Met1?) (Fig. 1). Sanger sequencing was performed and confirmed that none of the family members, except for the patient, carried this variant (Fig. 2). Further, the variant was novel against all public databases, including the Genome Aggregation Database (Karczewski et al. 2021), GenomeAsia 100K Project (GenomeAsia 2019), 1000 Genomes Project (Fairley et al. 2020), Trans-Omics for Precision Medicine program (Taliun et al. 2021), Greater Middle East Variome Project (Scott et al. 2016), Gutenberg Heart Study (Zeller et al. 2010), and the Qatar Genome Program (Mbarek et al. 2021).

As the patient has multiple features that fit MFDM (Table 1), we sought to examine the potential consequence of the variant on the expression of *EFTUD2*. Taking into consideration the relatively easier clinical accessibility to whole blood than other tissues, and that *EFTUD2* is well-expressed in this tissue (GTEx Consortium 2013), we used white blood cells to extract RNA and perform total RNA sequencing (RNA-seq) for each individual within the family. The data was normalized against RNA-seq profiles collected in our laboratory. The results indeed supported a decrease of *EFTUD2* expression in the proband, compared to all controls, including both parents and unaffected sibling (Fig. 3). These results support the pathogenicity of this variant causing a loss-of-function allele, and thus a drastic reduction in the expression of *EFTUD2* in vivo, leading to this syndromic phenotype.

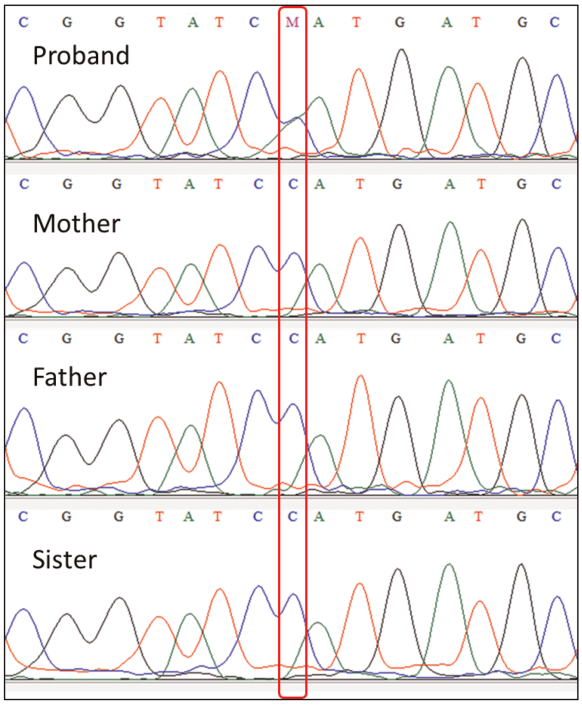

Figure 2. Sanger sequencing validation of the variant. The variant allele appears only in the proband. The M represents A or C, according to the IUPAC nucleotide codes.

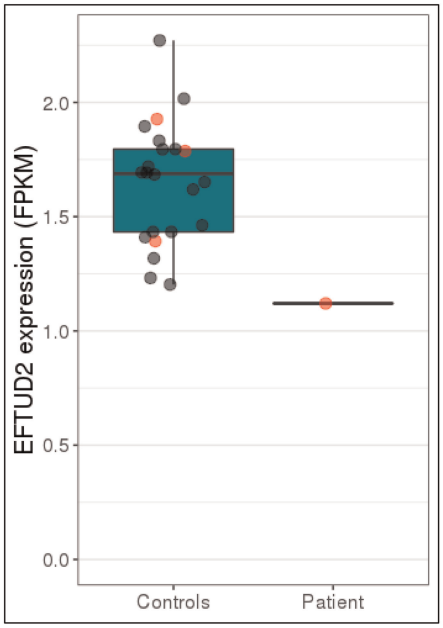

Figure 3. RNA-seq analysis of the *EFTUD2*. The boxplot shows FPKM (fragments per kilobase of transcript per million fragments)-normalized gene expression of EFTUD2 in patient versus healthy controls. Red dots indicate the sample of the patient (*right*) and her family (*left*).

DISCUSSION

Advancements in next-generation sequencing are paving the way to diagnose many previously idiopathic genetic conditions. Although prioritization and interpretation of the massive amounts of sequencing data is considered a challenge, the availability of public databases enhances the analysis of variations with regard to their putative role, functional impact, and contribution to human disease.

Here, we report a de novo variant in the start codon of the *EFTUD2*, which was predicted as damaging (CADD = 26.3) and occurs in a highly conserved region (GERP = 5.24). According to the American College of Medical Genetics and Genomics (ACMG) guidelines for the interpretation of sequence variants (Richards et al. 2015), multiple evidence lines support the pathogenicity of this variant. These include being a start-codon variant (PVS1), a de novo variant with confirmed paternity and maternity (PS2), and absent from controls in exome and genome databases (PM2). In addition, this variant affects a known dominant disease gene, *EFTUD2*, which plays a role in MFDM, further supporting this variant's pathogenicity in this patient.

The AUG start codon encodes the amino acid methionine and is responsible for the translation initiation, and therefore critical for production of a functional protein. A substitution affecting the putative start codon is predicted to cause a loss-of-function allele, which *ETUFD2* is predicted not to tolerate (probability of loss-of-function intolerance [pLI] > 0.99).

Evidence from the literature illustrated the important role of start-codon mutations in the development of different disease phenotypes (Ounap et al. 2012; Carrera et al. 2019; Lu et al. 2021; Xu et al. 2021b; Yang et al. 2021). However, it has also been proposed that the existence of close alternative start sites may enable protein translation and mitigate the effect of start-codon mutations (Abad-Navarro et al. 2018). To investigate this, we have examined the sequence downstream to the wild-type start codon and found an AUG triplet 14 bp away from the main start site. However, this site is missing a Kozak sequence and would cause a frameshift (Kozak 1986; Abad-Navarro et al. 2018), whereas the next closest alternative start site with a possible Kozak sequence occurs 922 bp away, within the following intron.

Mutations in the start codon render the ribosomes to search for alternative start sites for mRNA translation. These alternate start codons can be out of frame and may lead to a premature termination, which in turn leads to the degradation of the transcript by nonsense-mediated decay (Peccarelli and Kebaara 2014). Indeed, we performed RNA sequencing and measured the expression of *EFTUD2*, which confirmed the relatively decreased mRNA levels of *EFTUD2* in the patient, compared to the rest of the family and other controls, consistent with predicted loss-of-function impact of the start-codon variant on the gene expression.

In conclusion, we report a pediatric case with symptoms resembling MFDM, with a start-codon-loss mutation in the *EFTUD2*. To the best of our knowledge, this is the first study to report a start-codon loss in *EFTUD2* associated with MFDM, and it also expands the phenotypic spectrum of *EFTUD2*.

METHODS

Whole-Genome DNA and RNA Sequencing

Whole-blood samples were collected and total genomic DNA was extracted from each sample using DNeasy Blood & Tissue Kit (QIAGEN). Whole-genome libraries were prepared using TruSeq DNA Nano kit (Illumina), and samples were sequenced to an average depth of 30× using Illumina HiSeq X to produce 150-bp-length reads. For RNA sequencing, total

RNA extraction was carried out for each sample using the RNeasy Mini Kit (QIAGEN). After library preparation, samples were sequenced using Illumina HiSeq X.

Bioinformatic Analysis

After DNA sequencing, raw reads were aligned to GRCh37 reference genome using the standard settings of BWA kit v0.7.15 (Li and Durbin 2009). Pre- and postalignment genotype quality checks were performed to ensure high sample quality. For variant calling, we developed a combinatorial approach (M Kohailan W Aamer, N Syed, et al., unpubl.) to filter for de novo variants. Briefly, we used FreeBayes v1.1.0 (Garrison and Marth 2012), VarScan v2.3.9 (Koboldt et al. 2012), and RUFUS v1.0 (Farrell 2014) for the initial variant calling. Then, we combined the variants from all tools and applied more stringent filtration thresholds for variants unique to each tool. As a final step, we annotated variants using SnpEff 4.3T (Cingolani et al. 2012) and filtered out variants with an allele frequency of >0.1% in different databases (Zeller et al. 2010; Scott et al. 2016; GenomeAsia 2019; Fairley et al. 2020; Karczewski et al. 2021; Mbarek et al. 2021; Taliun et al. 2021). Raw reads were visualized with IGV software v2.9.4 (Robinson et al. 2011). For RNA sequencing, the differential gene expression analysis was performed using the R package DESeq2 v1.24 (Love et al. 2014).

Sanger Sequencing

The isolated DNA samples were used to amplify a 113-bp DNA sequence flanking the variant site using the Hot StarTaq Master Mix Kit (QIAGEN). Primer sequences were as follows: forward (5′-TCAGAATCAAGCTCTGGTCCAA-3′) and reverse (5′-AGGCCTTGATTACCT TGTCAGA-3′). After polymerase chain reaction (PCR) product purification with ExoSAP (Applied Biosystems), chain-termination and labeling reactions were performed using BigDye v3.1 Cycle sequencing kit (Life Technologies). Another product purification step was done using DyeEx plates (QIAGEN). Reactions were then loaded into the ABI 3500xl genetic analyzer (Life Technologies) to read the amplicon sequence.

ADDITIONAL INFORMATION

Data Deposition and Access

The variant was deposited in ClinVar (https://www.ncbi.nlm.nih.gov/clinvar/) under the accession number SCV002499764. The genomic sequence data we examined cannot be deposited because of institutional review board (IRB) restrictions and patient privacy.

Ethics Statement

The family (including proband, unaffected sister, and both parents) was enrolled for research by written informed consent, under IRB protocol IRB#1610004943 at Sidra Medicine.

Competing Interest Statement

The authors have declared no competing interest.

Referees

Saquib A. Lakhani
Anonymous

Received February 24, 2022; accepted in revised form May 2, 2022.

Acknowledgments

We thank the family that participated in this study. We also thank the Integrated Genomics Core at Sidra Medicine for performing whole-genome DNA and RNA Sequencing.

Author Contributions

A.K. diagnosed the patient; O.A. and A.A.A. recruited the patient to research; N.E. and W.A. processed the sample; S.P. performed the wet-lab validation; M.K. performed the bioinformatic analyses; and M.K. and K.F. wrote and submitted the manuscript.

Funding

This study is funded by the National Priorities Research Program (NPRP) of Qatar National Research Fund under grant number NPRP11S-0110-180250.

REFERENCES

Abad-Navarro F, de la Morena-Barrio ME, Fernández-Breis JT, Corral J. 2018. Lost in translation: bioinformatic analysis of variations affecting the translation initiation codon in the human genome. *Bioinformatics* **34:** 3788–3794. doi:10.1093/bioinformatics/bty453

Al-Kurbi AA, Da'as SI, Aamer W, Krishnamoorthy N, Poggiolini I, Abdelrahman D, Elbashir N, Al-Shabeeb Akil A, Glass GE, Fakhro KA. 2022. A recessive variant in *SIM2* in a child with complex craniofacial anomalies and global developmental delay. *Eur J Med Genet* **65:** 104455. doi:10.1016/j.ejmg.2022.104455

Beauchamp MC, Djedid A, Bareke E, Merkuri F, Aber R, Tam AS, Lines MA, Boycott KM, Stirling PC, Fish JL, et al. 2021. Mutation in *Eftud2* causes craniofacial defects in mice via mis-splicing of *Mdm2* and increased P53. *Hum Mol Genet* **30:** 739–757. doi:10.1093/hmg/ddab051

Carrera S, Beristain E, Sancho A, Iruarrizaga E, Rivero P, Mañe JM, López Vivanco G. 2019. Germline c.1A>C heterozygous pathogenic variant in *SDHA* reported for the first time in a young adult with a gastric gastrointestinal stromal tumour (GIST): a case report. *Hered Cancer Clin Pract* **17:** 23. doi:10.1186/s13053-019-0124-6

Cingolani P, Platts A, Wang le L, Coon M, Nguyen T, Wang L, Land SJ, Lu X, Ruden DM. 2012. A program for annotating and predicting the effects of single nucleotide polymorphisms, SnpEff: SNPs in the genome of *Drosophila melanogaster* strain w1118; iso-2; iso-3. *Fly (Austin)* **6:** 80–92. doi:10.4161/fly.19695

Deml B, Reis LM, Muheisen S, Bick D, Semina EV. 2015. *EFTUD2* deficiency in vertebrates: identification of a novel human mutation and generation of a zebrafish model. *Birth Defects Res A Clin Mol Teratol* **103:** 630–640. doi:10.1002/bdra.23397

Fabrizio P, Laggerbauer B, Lauber J, Lane WS, Lührmann R. 1997. An evolutionarily conserved U5 snRNP-specific protein is a GTP-binding factor closely related to the ribosomal translocase EF-2. *EMBO J* **16:** 4092–4106. doi:10.1093/emboj/16.13.4092

Fairley S, Lowy-Gallego E, Perry E, Flicek P. 2020. The International Genome Sample Resource (IGSR) collection of open human genomic variation resources. *Nucl Acids Res* **48:** D941–D947. doi:10.1093/nar/gkz836

Fakhro KA, Robay A, Rodrigues-Flores JL, Mezey JG, Al-Shakaki AA, Chidiac O, Stadler D, Malek JA, Imam AB, Sheikh A, et al. 2019. Point of care exome sequencing reveals allelic and phenotypic heterogeneity underlying Mendelian disease in Qatar. *Hum Mol Genet* **28:** 3970–3981. doi:10.1093/hmg/ddz134

Farrell JAR. 2014. Expanding the horizons of next generation sequencing with RUFUS. Doctor of Philosophy, The Graduate School of Arts and Sciences, Boston College.

Garison E, Marth G. 2012. Haplotype-based variant detection from short-read sequencing. arXiv: 1207.3907 doi:10.48550/arXiv.1207.3907

GenomeAsia KC. 2019. The GenomeAsia 100K Project enables genetic discoveries across Asia. *Nature* **576:** 106–111. doi:10.1038/s41586-019-1793-z

GTEx Consortium. 2013. The Genotype-Tissue Expression (GTEx) project. *Nat Genet* **45:** 580–585. doi:10.1038/ng.2653

Guion-Almeida ML, Zechi-Ceide RM, Vendramini S, Ju Nior AT. 2006. A new syndrome with growth and mental retardation, mandibulofacial dysostosis, microcephaly, and cleft palate. *Clin Dysmorphol* **15:** 171–174. doi:10.1097/01.mcd.0000220603.09661.7e

Guion-Almeida ML, Vendramini-Pittoli S, Passos-Bueno MR, Zechi-Ceide RM. 2009. Mandibulofacial syndrome with growth and mental retardation, microcephaly, ear anomalies with skin tags, and cleft palate in a mother and her son: autosomal dominant or X-linked syndrome? *Am J Med Genet A* **149A:** 2762–2764. doi:10.1002/ajmg.a.32816

Huang L, Vanstone MR, Hartley T, Osmond M, Barrowman N, Allanson J, Baker L, Dabir TA, Dipple KM, Dobyns WB, et al. 2016. Mandibulofacial dysostosis with microcephaly: mutation and database update. *Hum Mutat* **37:** 148–154. doi:10.1002/humu.22924

Jacob A, Pasquier J, Carapito R, Aurade F, Molitor A, Froguel P, Fakhro K, Halabi N, Viot G, Bahram S, et al. 2020. A *de novo* synonymous variant in EFTUD2 disrupts normal splicing and causes mandibulofacial dysostosis with microcephaly: case report. *BMC Med Genet* **21:** 182. doi:10.1186/s12881-020-01121-y

Karczewski KJ, Francioli LC, Tiao G, Cummings BB, Alfoldi J, Wang Q, Collins RL, Laricchia KM, Ganna A, Birnbaum DP, et al. 2021. The mutational constraint spectrum quantified from variation in 141,456 humans. *Nature* **590:** E53. doi:10.1038/s41586-020-03174-8

Kim SY, Lee DH, Han JH, Choi BY. 2020. Novel splice site pathogenic variant of *EFTUD2* is associated with mandibulofacial dysostosis with microcephaly and extracranial symptoms in Korea. *Diagnostics (Basel)* **10:** 296. doi:10.3390/diagnostics10050296

Koboldt DC, Zhang Q, Larson DE, Shen D, McLellan MD, Lin L, Miller CA, Mardis ER, Ding L, Wilson RK. 2012. VarScan 2: somatic mutation and copy number alteration discovery in cancer by exome sequencing. *Genome Res* **22:** 568–576. doi:10.1101/gr.129684.111

Kozak M. 1986. Point mutations define a sequence flanking the AUG initiator codon that modulates translation by eukaryotic ribosomes. *Cell* **44:** 283–292. doi:10.1016/0092-8674(86)90762-2

Lacour JC, McBride L, St Hilaire H, Mundinger GS, Moses M, Koon J, Torres JI, Lacassie Y. 2019. Novel de novo *EFTUD2* mutations in 2 cases with MFDM, initially suspected to have alternative craniofacial diagnoses. *Cleft Palate Craniofac J* **56:** 674–678. doi:10.1177/1055665618806379

Li H, Durbin R. 2009. Fast and accurate short read alignment with Burrows–Wheeler transform. *Bioinformatics* **25:** 1754–1760. doi:10.1093/bioinformatics/btp324

Li X, Hong M, Dai P, Yuan Y. 2022. Clinical case analysis and literature review of mandibulofacial dysostosis with microcephaly syndrome. *Lin Chung Er Bi Yan Hou Tou Jing Wai Ke Za Zhi* **36:** 36–40.

Love MI, Huber W, Anders S. 2014. Moderated estimation of fold change and dispersion for RNA-seq data with DESeq2. *Genome Biol* **15:** 550. doi:10.1186/s13059-014-0550-8

Lu XG, Yu U, Han CX, Mai JH, Liao JX, Hou YQ. 2021. c.3G>A mutation in the *CRYAB* gene that causes fatal infantile hypertonic myofibrillar myopathy in the Chinese population. *J Integr Neurosci* **20:** 143–151. doi:10.31083/j.jin.2021.01.267

Matsuo M, Yamauchi A, Ito Y, Sakauchi M, Yamamoto T, Okamoto N, Tsurusaki Y, Miyake N, Matsumoto N, Saito K. 2017. Mandibulofacial dysostosis with microcephaly: a case presenting with seizures. *Brain Dev* **39:** 177–181. doi:10.1016/j.braindev.2016.08.008

Mbarek H, Gandhi GD, Selvaraj S, Al-Muftah W, Badji R, Al-Sarraj Y, Saad C, Darwish D, Alvi M, Fadl T, et al. 2021. Qatar genome: insights on genomics from the Middle East. *Hum Mutat* **43:** 499–510. doi:10.1002/humu.24336

Narumi-Kishimoto Y, Ozawa H, Yanagi K, Kawai T, Okamura K, Hata K, Kaname T, Matsubara Y. 2020. A novel *EFTUD2* mutation identified an adult male with mandibulofacial dysostosis Guion-Almeida type. *Clin Dysmorphol* **29:** 186–188. doi:10.1097/MCD.0000000000000330

Ounap K, Puusepp-Benazzouz H, Peters M, Vaher U, Rein R, Proos A, Field M, Reimand T. 2012. A novel c.2T>C mutation of the *KDM5C/JARID1C* gene in one large family with X-linked intellectual disability. *Eur J Med Genet* **55:** 178–184. doi:10.1016/j.ejmg.2012.01.004

Peccarelli M, Kebaara BW. 2014. Regulation of natural mRNAs by the nonsense-mediated mRNA decay pathway. *Eukaryot Cell* **13:** 1126–1135. doi:10.1128/EC.00090-14

Rengasamy Venugopalan S, Farrow EG, Lypka M. 2017. Whole-exome sequencing identified a variant in *EFTUD2* gene in establishing a genetic diagnosis. *Orthod Craniofac Res* **20:** 50–56. doi:10.1111/ocr.12150

Richards S, Aziz N, Bale S, Bick D, Das S, Gastier-Foster J, Grody WW, Hegde M, Lyon E, Spector E, et al. 2015. Standards and guidelines for the interpretation of sequence variants: a joint consensus recommendation of the American College of Medical Genetics and Genomics and the Association for Molecular Pathology. *Genet Med* **17:** 405–424. doi:10.1038/gim.2015.30

Robinson JT, Thorvaldsdottir H, Winckler W, Guttman M, Lander ES, Getz G, Mesirov JP. 2011. Integrative Genomics Viewer. *Nat Biotechnol* **29:** 24–26. doi:10.1038/nbt.1754

Scott EM, Halees A, Itan Y, Spencer EG, He Y, Azab MA, Gabriel SB, Belkadi A, Boisson B, Abel L, et al. 2016. Characterization of Greater Middle Eastern genetic variation for enhanced disease gene discovery. *Nat Genet* **48:** 1071–1076. doi:10.1038/ng.3592

Silva JB, Soares D, Leao M, Santos H. 2019. Mandibulofacial dysostosis with microcephaly: a syndrome to remember. *BMJ Case Rep* **12:** e229831. doi:10.1136/bcr-2019-229831

Taliun D, Harris DN, Kessler MD, Carlson J, Szpiech ZA, Torres R, Taliun SAG, Corvelo A, Gogarten SM, Kang HM, et al. 2021. Sequencing of 53,831 diverse genomes from the NHLBI TOPMed Program. *Nature* **590:** 290–299. doi:10.1038/s41586-021-03205-y

Wieczorek D, Shaw-Smith C, Kohlhase J, Schmitt W, Buiting K, Coffey A, Howard E, Hehr U, Gillessen-Kaesbach G. 2007. Esophageal atresia, hypoplasia of zygomatic complex, microcephaly, cup-shaped ears, congenital heart defect, and mental retardation—new MCA/MR syndrome in two affected sibs and a mildly affected mother? *Am J Med Genet A* **143A:** 1135–1142. doi:10.1002/ajmg.a.31752

Wieczorek D, Gener B, Gonzalez MJ, Seland S, Fischer S, Hehr U, Kuechler A, Hoefsloot LH, de Leeuw N, Gillessen-Kaesbach G, et al. 2009. Microcephaly, microtia, preauricular tags, choanal atresia and

developmental delay in three unrelated patients: a mandibulofacial dysostosis distinct from Treacher Collins syndrome. *Am J Med Genet A* **149A:** 837–843. doi:10.1002/ajmg.a.32747

Xu BQ, Zhen L, Li DZ. 2021a. First-trimester detection of micrognathia as a presentation of mandibulofacial dysostosis with microcephaly. *J Obstet Gynaecol* **41:** 821–823. doi:10.1080/01443615.2020.1785410

Xu X, Zhao J, Wang C, Qu X, Ran M, Ye F, Shen M, Wang K, Zhang Q. 2021b. Case report: de novo *KLHL24* gene pathogenic variants in Chinese twin boys with epidermolysis bullosa simplex. *Front Genet* **12:** 729628. doi:10.3389/fgene.2021.729628

Yang L, Lu G, Shen W, Chen W, Lu H, Zhang G, Yuan S, Zheng S, Ren J. 2021. Whole-exome sequencing of a novel initiation codon mutation in *RUNX2* in a Chinese family with cleidocranial dysplasia. *Medicine (Baltimore)* **100:** e27746. doi:10.1097/MD.0000000000027746

Yu KPT, Luk HM, Gordon CT, Fung G, Oufadem M, Garcia-Barcelo MM, Amiel J, Chung BHY, Lo IFM, Tiong YT. 2018. Mandibulofacial dysostosis Guion-Almeida type caused by novel *EFTUD2* splice site variants in two Asian children. *Clin Dysmorphol* **27:** 31–35. doi:10.1097/MCD.0000000000000214

Zeller T, Wild P, Szymczak S, Rotival M, Schillert A, Castagne R, Maouche S, Germain M, Lackner K, Rossmann H, et al. 2010. Genetics and beyond—the transcriptome of human monocytes and disease susceptibility. *PLoS ONE* **5:** e10693. doi:10.1371/journal.pone.0010693